Materials Horizons

Accepted Manuscript

This article can be cited before page numbers have been issued, to do this please use: C. Izquierdo, E. Fresta, E. Serrano, E. Lalinde Peña, J. Garcia-Martinez, J. R. R. Berenguer and R. D. Costa, *Mater. Horiz.*, 2018, DOI: 10.1039/C8MH00578H.

ROYAL SOCIETY OF CHEMISTRY

rsc.li/materials-horizons

View Article Online
DOI: 10.1039/C8MH00578H

White hybrid light-emitting diodes (WHLEDs) combine a high-energy emitting LED with low-energy emitting organic color down-converting packings, which are easy-to-prepare and eco-friendly. Here, one of the most outstanding down-converting materials are luminescent organometallo-silica nanoparticles. Up to date, the synthesis methodology has been limited by the incorporation of a single complex, leading to a moderate color stability in WHLEDs due to different aging rates. Herein, we disclose a new synthesis protocol based on the kinetic control of the formation of organometallic dots with three emitting iridium(III) complexes, which are subsequently transformed into mesoporous silica nanoparticles. The white organometallo-silica nanoparticles show record photoluminescence quantum yields stable under severe scenarios. Noteworthy, WHLEDs prepared with this novel down-converting material provide encouraging proof-of-concept performances including a stable (>1000h) emission with a sun-like spectrum.

View Article Online
DOI: 10.1039/C8MH00578H

"for Table of Contents only"

White-emitting organometallo-silica nanoparticles for sun-like light-emitting diodes

C. Ezquerro,[a] E. Fresta,[b] E. Serrano,[c] E. Lalinde,[a] J. García-Martínez*[c], J. R. Berenguer*[a] and R. D. Costa*[b]

All for one and one for all! First white-emitting organometallo-silica nanoparticles, based on the formation of organometallic dots (**OD**s) made of a mixture of blue-, green- and red-emitting complexes, show excellent photo- and thermal-stabilities. They have been applied to design one of the most stable single-component white emitting hybrid light-emitting diodes that closely mimics the sunlight.

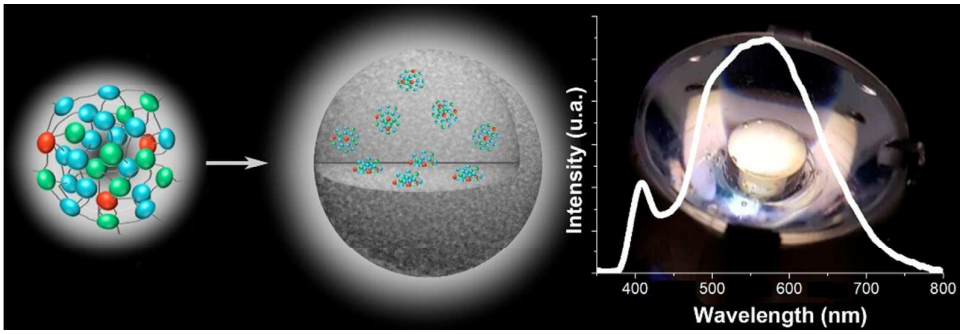

View Article Online
DOI: 10.1039/C8MH00578H

Materials Horizons

COMMUNICATION

White-emitting organometallo-silica nanoparticles for sun-like light-emitting diodes

Cintia Ezquerro,[a]† Elisa Fresta,[b]† Elena Serrano,[c] Elena Lalinde,[a] Javier García-Martínez,[c]* Jesús R. Berenguer,[a]* and Rubén D. Costa[b]*

Received 00th January 20xx,
Accepted 00th January 20xx

DOI: 10.1039/x0xx00000x

www.rsc.org/

This work discloses a radically new way to prepare white-emitting hybrid nanoparticles, whose implementation in lighting devices provides encouraging proof-of-concept performances towards alternative sunlight sources. In detail, the new synthetic approach is based on the kinetic control of the formation of organometallic dots, built *via* the condensation of three emitting iridium(III) complexes, which are subsequently transformed into mesoporous silica nanoparticles. Our novel hybrid systems, which are exceptionally stable under harsh irradiation and thermal stress environments, show a bright white emission with a record photoluminescence quantum yield. Their remarkable performance prompted us to implement them into single-component hybrid light-emitting diodes (HLEDs), achieving a high-quality sunlight source that is stable >2000 hours with linearly extrapolated stabilities >10000 h. This represents one of the most stable HLEDs reported so far, while the versatility of our synthesis approach with respect to the type of emitters opens new opportunities for the design and fabrication of white-emitting color down-converters for HLEDs of the future.

INTRODUCTION

To design the next generation of artificial illumination, two main routes have been developed. In a first approach, white organic light-emitting diodes (WOLEDs) have raised great expectations in both industrial and scientific communities.[1] However, they require a multilayered structure based on several organic semiconductors, which are needed for charge injection, charge transport/blocking, and light emission.[2] Although there are large-area devices featuring luminous efficiencies of 50-60 lm/W and stabilities of thousands of hours,[2a] this is not sufficient for their large scale application as it is still necessary to develop i) simple architectures to enhance charge transport and recombination, as well as light out-coupling, ii) stable blue emitters, and iii) easy and low-cost fabrication processes.[2a, 2b] In a second approach, all-inorganic white light-emitting diodes (IWLEDs) are dominating the lighting market. IWLEDs are highly efficient UV- or blue-emitting inorganic chips covered by color down-converting coatings that partially transform the high-energy chip emission into visible light.[1, 3] The most widely used color down-converters are based on yellow-emitting rare-earth doped crystals, such as cerium-doped yttrium aluminium garnet ($Y_3Al_5O_{12}$:Ce^{3+}; YAG:Ce).[4] They feature excellent photo- and thermal-stabilities, high photon flux saturations and photoluminescence quantum yields (ϕ)>70%. However, reliance on rare-earth materials implies high production costs, as well as uncertain availability. In addition, and despite many efforts, the possibility to use chemical routes to tune the color emission of these compounds is still a challenge, which greatly limits the LED color quality of these systems.[1, 3-4] Certainly, this is a major concern, because the high blue-light component is hazardous for the human retina of both children and elders, the circadian cycle, and the hormonal system.[5] Hence, much effort is put into enhancing the white light quality of LEDs by better mimicking natural sunlight.[5]

[a] *Departamento de Química-Centro de Investigación en Síntesis Química (CISQ), Universidad de La Rioja, Madre de Dios, 53, E-26006, Logroño, La Rioja (Spain). E-mail: jesus.berenguer@unirioja.es*
[b] *IMDEA Materials Institute, Calle Eric Kandel 2, E-28906 Getafe, Madrid (Spain). E-mail: ruben.costa@imdea.org*
[c] *Laboratorio de Nanotecnología Molecular, Departamento de Química Inorgánica, Universidad de Alicante, Ctra. Alicante-S. Vicente s/n, E-03080 Alicante (Spain). E-mail: j.garcia@ua.es*
† These authors contributed equally to this work.
Electronic Supplementary Information (ESI) available: [Full experimental procedures and theoretical calculations of complexes **B** and **R**. Textural and morphological characterization of nanoparticles. Photophysical properties of complexes, nanoparticles and rubbers-like materials. Fabrication, characterization and photostability measurements of WHLEDs]. See DOI: 10.1039/x0xx00000x

View Article Online
DOI: 10.1039/C8MH00578H

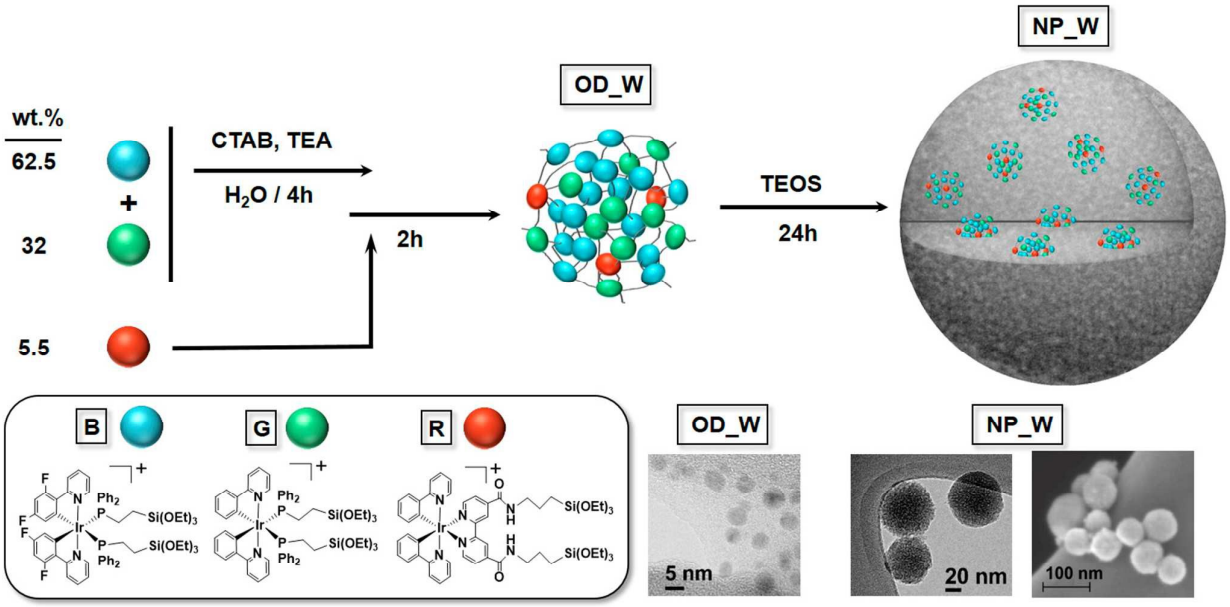

Scheme 1. Schematic representation of the synthesis of white-emitting organometallic dots (**OD_W**) and nanoparticles (**NP_W**) using blue-, green-, and red-emitting alkoxysilane-based Ir(III) complexes (**B**, **G**, **R**, respectively). Pictures showing Transmission Electron Microscopy (TEM) photographs of both types of nanomaterials and Field-Emission Scanning Electron Microscopy (FESEM) image of **NP_W**.

The current limitations in the development of high quality lighting systems has, therefore, encouraged further efforts to produce hybrid inorganic/organic WLED architectures (HWLED).[6] Here, organic or inorganic color down-converters, such as polymers, coordination complexes, carbon nanodots or fluorescent proteins, have been tested in new packaging matrices like polymers, cellulose, metal organic frameworks (MOFs), *etc*.[7] State-of-the-art HWLEDs involve luminous efficiencies up to 120 lm/W and high color quality with x/y CIE color coordinates of 0.30-3/0.30-3, color rendering index (CRI) above 80-90, and correlated color temperatures (CCT) ranging from 2700 K to 6500 K. Their major drawback is the device stability, which is typically limited to a maximum of few hundred hours.[6-7] Among the color down-converters above mentioned, organometallic complexes stand out.[7i, 7k, 7m, 8]

In light of the aforementioned, there are two major challenges for the preparation of high quality and stable HWLEDs. On the one hand, it is highly desirable to develop new color down-converting coatings with enhanced photostabilities and thermal management, which will allow for high irradiation intensities under ambient conditions. On the other hand, there is a strong need of white-emitting single-component down-converting coatings. The use of mixtures of emitters leads to a loss of performance stemming from i) reabsorption, ii) phase separation over time, and iii) poor color stability due to differences in both thermal quenching and aging rates of the emitters.

Tackling both challenges simultaneously constitutes the major thrust of the work at hand. Our approach builds on the synthetic strategies developed to modify silica nanoparticles *via* encapsulation or grafting of a myriad of chromophores, which have produced highly promising results. These studies include perovskite nanocrystals, quantum dots, organic dyes or carbon nanodots.[9] In an effort to better integrate the active moiety in the silica matrix, we[10] and others[7m, 11] have developed the so-called Sol-Gel Coordination Chemistry, which is based on the co-condensation of an emissive organometallic complex bearing alkoxysilane terminal groups with a silica source – *i.e.* tetraethyl orthosilicate (TEOS). This approach allows for preparing hybrid materials with the chromophore homogeneously incorporated into the silica framework. Recently, this strategy has been also used to obtain luminescent organometallo-silica nanoparticles featuring enhanced stability and photophysical properties compared to those of the complexes.[10] However, up to date, this methodology has been focused only on the incorporation of a single organometallic complex.[7m, 11-12]

Herein, we report a novel strategy for the synthesis of the first white-emitting organometallo-silica nanoparticles, in which blue-, green-, and red-emitting organometallic Ir(III) complexes are simultaneously encapsulated (*three-in-one*) *via* sol-gel inside silica nanoparticles. A key aspect of our synthetic approach is the kinetic control of the formation of the white-emitting organometallic dots (**OD**), built prior to the growth of the silica nanoparticle (**NP**). But the most remarkable contribution of our method is that the combination of the emission characteristics of the three complexes leads to an exceptionally high quality white emission that is stable under harsh environments. As such, the white-emitting nanoparticles have been used as color down-converters to develop single-component HWLEDs, featuring excellent color quality (sun-like light) that are stable over thousands of hours (>2000 h continuous and >10000h using a linear extrapolation up to 50% brightness) measured in air. While their performance stands out among the state-of-the-art HWLEDs,[6-7] this works presents an original and versatile synthesis approach to design highly emissive white emitters, which paves the road for future breakthroughs in the HWLED field.

View Article Online
DOI: 10.1039/C8MH00578H

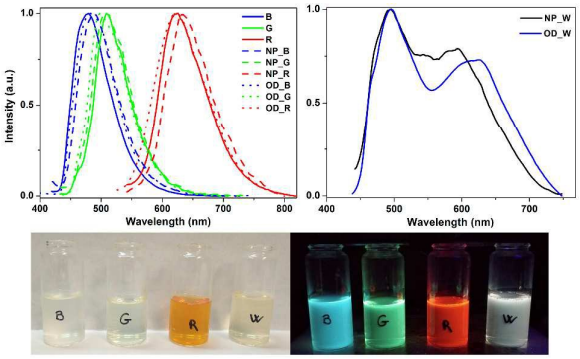

Figure 1. Upper part – Left: Emission spectra (λ_{exc}=365 nm for **B** and **G**; λ_{exc}=470 nm for **R**) at room temperature of complexes **B**, **G**, **R** in solid-state (solid line), their respective monochromatic emitters **OD** in suspension (dotted line), and **NP** in solid-state (dashed line). Right: Emission spectra (λ_{exc}=390 nm) at room temperature of the white emitting **OD_W** and **NP_W** in suspension and solid-state, respectively. Lower part – Pictures of suspensions of the organometallic dots **OD** in the reaction media under room light (left) and UV irradiation (365 nm, 4 W) illumination (right).

RESULTS

Synthesis and photophysical properties of the organometallic precursors

To prepare the white-emitting organometallo-silica nanoparticles, we focused on cyclometalated Ir(III) complexes, which are currently among the most efficient, stable, and emission tunable color phosphorescent emitters.[13] In detail, we have recently reported the bis-phosphine complex $[Ir(ppy)_2(PPETS)_2]OTf$ (**G**) [ppy= 2-phenylpyridinyl, PPETS = $PPh_2(CH_2)_2Si(OEt)_3$][10a] – Scheme 1 – which features a green unstructured emission band in solid-state (298 K) – Fig. 1; maximum emission wavelength or λ_{em}=512 nm, ϕ=31.2%, excited-state lifetime or τ=0.97 μs – associated to a triplet excited state with a mixed ^{3}ILCT(ppy)/^{3}MLCT(Ir → ppy) nature – *i.e.*, ILCT refers to intra-ligand charge transfer and MLCT refers to metal-to-ligand charge transfer. Blue emission was attained using the dfppy ligand to obtain the complex $[Ir(dfppy)_2(PPETS)_2]PF_6$ (**B**) [dfppy= 2-(2,4-difluorophenyl)pyridinyl] – Scheme 1. The latter exhibits a blue-shifted emission in solid-state (298 K) – Fig. 1; λ_{em}=480 nm, ϕ=23.5%, τ=1.55 μs – also ascribed to a triplet excited state with a mixed ^{3}ILCT(dfppy)/^{3}MLCT(Ir → dfppy) nature.

Finally, the red-emitting chromophore was obtained by replacing the PPETS ligands of the **G** derivative by a bipyridine ligand bearing two alkoxysilane groups – *i.e.*, dasipy= 4,4'-$[CONH(CH_2)_3Si(OEt)_3]$-bipyridine. As expected, the resulting complex $[Ir(ppy)_2(dasipy)]OTf$ (**R**; Scheme 1) shows a red emission in solid-state (298 K) – Fig. 1; λ_{em}=620 nm, ϕ=16.5%, τ=0.13 μs – attributed to a triplet excited state with a mixed ^{3}ML'CT(Ir → dasipy)/^{3}LL'CT(ppy → dasipy) having a remarkable ML'CT character – *i.e.*, LL'CT refers to ligand-to-ligand charge transfer. The three alkoxysilane derivatives have been obtained from their respective solvato precursors – *i.e.*, $[Ir(ppy)_2(MeCN)_2]^+$ and $[Ir(dfppy)_2(MeCN)_2]^+$ – and fully characterized by the usual analytical and spectroscopic means, as well as theoretical calculations – see Experimental Procedures, Tables S1-S4 and Fig. S1-S6 in the supporting information (SI) for further details.

Preparation and characterization of the organometallo-silica nanoparticles.

The synthetic procedure to prepare the hybrid white-emitting organometallo-silica nanoparticles (**NP_W**) is based on a two-step sol-gel process and it was performed at room temperature. The white emission was achieved using an optimized content of the three Ir(III) complexes, namely 0.125 wt.% **B**, 0.064 wt.% **G**, and 0.011 wt.% **R**, which yields a mass ratio of 62.5 **B**: 32 **G**: 5.5 **R**. It should be noted that a low content of the red-emitting complex in the mixture was required, as the increase in the concentration of **R** always give rise to emissions with a majority contribution of the red component. This fact, and the good overlap between the low energy absorption feature of **R** and the emissions of complexes **B** and **G** in the solid state (450-550 nm, see Figure S7), point to the occurrence of a certain degree of energy transfer from the blue and green chromophores to the red one.

In detail, the three alkoxysilane derivatives **B**, **R**, **G** were firstly prehydrolyzed in an ethanolic-water mixture under kinetic control, in the presence of hexadecyltrimethylammonium bromide (CTAB) to moderate the growth of the organometallic dots formed (**OD_W**) – Scheme 1. Taking into account the different rates of hydrolysis of PPETS complexes when compared to the dasipy derivative, complexes **B** and **G** were firstly hydrolyzed for 4 h followed by the addition of **R**. The mixture was stirred for 2 additional hours – see SI for further details. In this way, the alkoxysilane groups of the complexes condensate under mild conditions forming small organometallic dots (**OD_W**) of about 5 nm in diameter as estimated by Transmission Electron Microscopy (TEM) – Scheme 1 and Fig. S8. According to their volume in relation with the average volume of the molecules of the organometallic complexes, the **OD_W** must be formed by less than 50 molecules that are covalently bonded together through Si-O bonds. The **OD_W** were then subjected to further sol-gel condensation with TEOS added to the reaction media and then reacted for 24 hours at room temperature, yielding the final hybrid white-emitting organometallo-silica nanoparticles **NP_W** – Scheme 1 and Fig. S9. Similarly, monochromatic emitting blue (**NP_B**), green (**NP_G**), and red (**NP_R**) hybrid silica nanoparticles, with a nominal iridium content of 0.2 wt.%, were also obtained from their respective **B**, **G**, and **R** complexes, through the previous formation of the corresponding **OD_B,G,R** organometallic dots – Scheme S1 and Fig. S9. Finally, Field Emission Scanning Electron Microscopy (FESEM) analysis of both the monochromatic **NP_B,G,R** and the white-emitting **NP_W** also corroborated nearly monodispersed spherical shape particles with sizes in the 50-70 nm range – Fig. S10 for **NP_W**. ICP analyses of these solids gave incorporation yields between 80-90% – Table S5.

View Article Online
DOI: 10.1039/C8MH00578H

Physisorption experiments were carried out to study the porosity of the organometallo-silica nanoparticles. For comparison purposes, the isotherm and pore size distribution of related organometallo-free silica nanoparticles (**Control NP**; see SI) are also included in Fig. S11. All samples yielded similar type IV isotherms with Brunauer–Emmett–Teller (BET) surface areas of *ca*. 1000 m^2/g and mesopore volumes in the 0.5-0.7 cm^3/g range – Fig. S11 and Table S5.[14] An additional adsorption process takes place at $P/P_0>0.8$, which is characteristic of interparticle porosity. Thanks to the use of CTAB as surfactant, the mesopores are quite homogeneous in size, as evidenced by their narrow pore size distribution with an average pore size in the 2.1-2.4 nm range – Fig. S11. This feature was also observed by TEM. Both the monochromatic **NP_B,G,R** and the white emitting **NP_W** nanoparticles showed the typical morphology of mesoporous discrete silica nanoparticles prepared in the presence of CTAB – Fig. S9. Moreover, both the mesopore volume and average mesopore diameter remained almost the same after incorporating the organometallic complexes into the silica **NP**s. This fact is consistent with the integration of the initially formed emissive **OD**s through the silica matrix,[10] and with the photophysical properties of the hybrid silica as described below.

The organometallo-silica nanoparticles **NP_B,G,R** and their corresponding dots **OD_B,G,R** display similar emission properties to those observed for the corresponding **B**, **G**, and **R** complexes in solid-state – Fig. 1, Fig. S12-S19, and Tables S6-S7. This indicates that the **OD**s are generated without any significant structural change of their constituent complexes. Notably, although smaller than those found for the pure complexes, the **NP_B,G,R** show ϕ ranging from 10 to 20 %.

In contrast, **NP_W** nanoparticles, which are formed from a mixture of the **B**, **G**, and **R** complexes in the appropriate mass content – *vide supra*, exhibit a white emission associated to a broad (full width at half maximum of *ca*. 6250 cm^{-1}) band with maxima at 490 and 595 nm along with a tail extending up to 750 nm – Fig. 1. Not unexpectedly, the photoluminescence response is excitation wavelength (λ_{exc}) dependent. As shown in Fig. S18 (right), the lowest energy emission feature intensifies upon exciting at lower energies. The excitation spectrum (Fig S18, left) monitored at the red low-energy emission peak (580 nm) shows a peak at 500 nm, which overlaps with the emission for both the blue and green emitters. This fact also suggests the occurrence of an energy transfer process from the high-energy emitting complexes to the red-emitting one inside the NP_W, as noted before on the basis of absorption and emission spectra (see Fig S7). Further confirmation was obtained upon comparing the τ values of **NP_W** monitored at 480 nm (0.57 μs), 510 nm (0.64 μs), and 595 (0.63 μs) with those of **NP_B** (0.99 μs), **NP_G** (0.89 μs), and **NP_R** (0.12 μs) at their respective emission maxima – Table S7. Here, the energy transfer process is pinpointed by the slight τ decrease of the blue and green emitters and a clear τ increase of the red one.[15] The variation in the excited state lifetimes suggests a certain degree of Förster resonance energy transfer. However, in multimetallic systems incorporating phosphorescent emitters (Ru(II), Os(II), Ir(III)), a significant triplet-triplet Dexter contribution to the energy transfer rate has been reported, although chromophores are not able to get a good conjugation in the ground state.[15b]

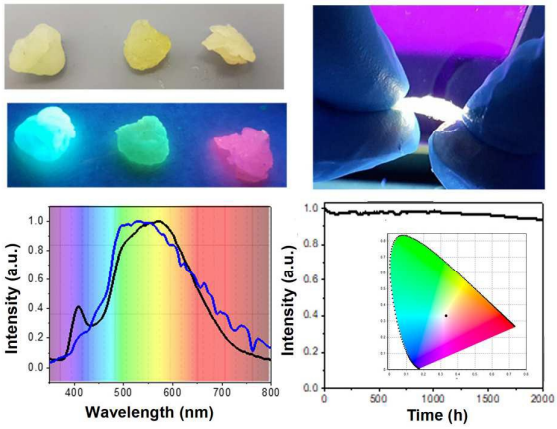

Figure 2. Upper part – Left: Picture of the monochromatic **NP_B,G,R** rubbers under room light (top) and UV (310 nm, 8 W) irradiation (bottom). Right: Picture of **NP_W** rubber under UV (310 nm, 8 W) irradiation. Lower part – Left: Electroluminescence spectrum of single-component WHLEDs compared with the visible part of the sunlight spectrum (measured in Madrid, 12/12/2017, h 13. Right: Changes of the luminous efficiency of the WHLEDs and the x/y CIE color coordinates (inset) over time under applied constant current of 150 mA.

In order to investigate the importance of having the three complexes in close proximity, we mixed the appropriate amounts of **NP_B**, **NP_G**, and **NP_R** nanoparticles**,** obtaining a homogeneous mixture with the same weight ratio of chromophores than in **NP_W**. As shown in Fig. S19, the mixture shows a weaker broad emission band, likely due to some degree of reabsorption, in which the low energy maximum (*ca*. 600 nm) is missing. Hence, the energy transfer is only feasible in a short distance range process – *i.e.*, the **OD_W** size of *ca*. 5 nm formed with the three complexes in the **NP_W** sample,[15a, 16] and it cannot happen in the homogeneous mixture of **NP_B**,**G**,**R**, where each single emitter is localized inside the silica nanoparticles, which are 50-70 nm in diameter. Indeed, similar emission properties were noted for the **OD_W** dots compared to that of the **NP_W** – Table S7 and Fig. S18-S19. All-in-all, the occurrence of a certain degree of energy transfer in the *in-situ* **OD_W** and **NP_W** from the blue and green chromophores to the red one explains the high contribution of the low energy emission, despite the small relative amount of **R** in the **NP_W** (5.5 wt.%). Noteworthy, the white emission is associated to a ϕ of 20.5 % (λ_{exc} = 390 nm), which represents one of the highest value reported for white emitting silica nanoparticles.[9a-e, 9g, 9i]

Design and study of HWLEDs

These findings encouraged us to shed light onto the prospect of the novel white-emitting hybrid silica nanoparticles as color down-converting coatings and/or packagings for HWLEDs. Following our previous reports,[18–20] both pure organometallic

View Article Online
DOI: 10.1039/C8MH00578H

complexes (**B**, **G**, **R**) and monochromatic emitting nanoparticles **NP_B**,**G**,**R** were implemented into a rubber-like coating – *i.e.*, hereafter **OC**- or **NP**-rubbers – based on a mixture of branched and linear poly(ethylene oxide) polymers – see Fig. 2 and SI for more details.

The photoluminescence features of these **OC**- and **NP**-rubbers (5 mm thick) were firstly investigated. Similar emission spectra to those observed for both **B**, **G** or **R** complexes and **NP_B,G,R** nanoparticles were noted – Fig. S20-S21, indicating that the emitter-matrix interaction is not very strong. Moreover, the rubbers show excellent photo- and thermal-stabilities under both ambient conditions and harsh environments, such as long-term storage, UV irradiation (310 nm, 8 W), and thermal treatment up to 70 °C – Fig. S20-S21. While all of them show excellent stabilities over months upon storage, rubbers with the emitting nanoparticles show superior photo- and thermal-stabilities – *i.e.,* no changes were observed under extreme conditions (UV irradiation at 70°C) compared to rubbers with only coordination complexes, which quickly degrade after a few hours – Fig. S20-S21.

Following these assays, we decided to fabricate a series of HLEDs using a commercial UV-LED with a 400 nm emitting chip – *i.e.*, WINGER® WEPUV3-S2 UV Power LED Star (Blacklight) 1.2W – covered by thick (1 mm) color down-converting coatings based on rubbers with the organometallic complexes (**OC**-HLEDs) and the monochromatic **NP_B**, **NP_G**, and **NP_R** hybrid nanoparticles (**NP**-HLEDs). These devices were driven (i) at different applied currents, to evaluate their color conversion properties, and (ii) at constant current, to determine the device stability. In both experiments, the changes in the overall spectrum, the luminous efficiency, and the temperature of the HLEDs were monitored – see SI for more details. Upon applying different currents ranging from 20 to 200 mA, the superior performance of **NP**-HLEDs was attested by the color down-conversion efficiency (η_{con}), which is defined as the ratio between the maxima of the down-converting and the LED emission bands – Fig. S22, while both **OC**- and **NP**-HLEDs showed a linear increase of the η_{con} *versus* applied current, indicating that there is no saturation, bleaching, and/or non-linear related quenching effects.

Next, the beneficial effect of incorporating the complexes into the silica nanoparticles during their synthesis was clearly revealed by the stability tests, which were performed at a constant applied current of 150 mA. As reference devices, blue and green **OC**-HLEDs showed luminous efficiencies of 0.27 and 1.65 lm/W, respectively. They show a quick degradation (blue **OC**-HLED) or exponential decrease (green **OC**-HLED) in luminous efficiency within the first hour – Fig. S23-S24. In addition, the emission maxima of the color down-conversion band for blue **OC**-HLEDs significantly changed from 495 to 520 nm, as well as x/y CIE color coordinates from 0.18/0.18 to 0.31/0.44 after 4 hours of operation. In contrast, red-emitting **OC**-HLEDs showed a stable emission spectrum during several hours – *i.e.*, maximum emission centered at 630 nm and x/y CIE color coordinates of 0.61/0.29– Fig. S25. This was associated to a low luminous efficiency of 0.03 lm/W. In stark contrast, the **NP**-HLEDs showed much higher and stable luminous efficiencies, reaching values of 1.24, 1.30, and 1.50 lm/W for blue-, green-, and red-emitting **NP**-HLED, respectively – Fig. S23-S25. Importantly, the temperature of the down-converting coatings reached 30-32°C for both **OC**- and **NP**-HLEDs. This fact strongly suggests that the main impact of the silica encapsulation is the isolation of the emitters from both the ambient oxygen and the residual solvent present in the matrix, as well as the geometry constrain of the organometallic molecules that limits non-radiative vibrational relaxation motion upon continuous excitation. Hence, the use of the hybrid NPs (**NP_B**,**G**,**R**) leads to HLEDs with enhanced luminous efficiency and stability features.

Similar to the **NP**-HLEDs, we fabricated single-component **NP**-HWLEDs using the **NP_W** nanoparticles. Remarkably, these devices showed a broad emission spectrum with a maximum at 590 nm close flanked by shoulders at *ca*. 500 and 620 nm, which perfectly matches with that of the natural sunlight measured in Madrid on December; 2017 – Fig. 2. Moreover, **NP**-HWLEDs showed minimal changes with respect to the emission spectrum at different measuring angles – Fig. S26, suggesting a uniform spherical light distribution. Finally, these devices show a remarkable stability over 2000 h under continuous operation conditions, while – Fig. 2. This is confirmed by the neglectable changes in luminous efficiency of 2.5 lm/W (<5% decrease) and constant x/y CIE color coordinates of 0.34/0.33, CRI of 85, and CCT of 5143 K, representing one of the most stable HWLEDs reported so far.[7b, 7d-f, 7i, 17] What is more, these devices can reach values of ca. 10000h of stability using a linear extrapolation up to 50% of the maximum luminance – Fig. S27. To highlight the importance of using a single-component device, we assembled related multi-component devices using a mixture of **NP_B**, **NP_G**, and **NP_R** with the same weight ratio to that of the organometallic complexes in **NP_W**. As expected, the lack of an efficient energy transfer between monochromatic NPs – *vide supra*, leads to devices failing to provide white light due to the lack of emission in the low-energy region – *i.e.*, λ>600nm, Fig. S28.

Conclusions

In conclusion, we have disclosed an innovative and efficient way of realizing the first white-emitting organometallo-silica nanoparticles. They have been obtained by kinetically controlling the covalent bonding at the molecular level of three different organometallic chromophores prior to the formation of the silica matrix around them. These white-emitting nanoparticles show a high photoluminescence quantum yield value (20%) that is stable over months under harsh environments. In addition, these white hybrid silica nanoparticles have been implemented into a rubber-like down-converting coating, achieving one of the most stable single-component HWLEDs up to date. Moreover, the excellent light distribution and color quality of the new HWLEDs was demonstrated by comparing it to the sunlight spectrum. As such, this work provides a ground-breaking contribution towards eye-friendly, exceptionally efficient, and

View Article Online
DOI: 10.1039/C8MH00578H

highly stable HWLEDs. These unique features, which are usually mutually exclusive, has been achieved thanks to the use of a new three-in-one approach that allows to overcome quenching, poor color stability, and phase separation issues, which are common drawbacks of organic color down-converting coatings for HWLEDs. Our strategy has successfully overcome these limitations by using white-emitting silica nanoparticles (**NP_W**), which combine a better preservation of the integrity of the complexes, thanks to geometry constraint produced by the silica matrix, and the proximity of the chromophores within the white-emitting organometallic dots (**OD_W**), which are incorporated within the protective silica shell.

Although the device stability values represent a breakthrough, the maximum efficiency is far from the state-of-the-art. A such, future work will be directed at obtaining organometallic complexes with higher photoluminescence quantum yields and closer surface nanoparticles to enhance the environmental protection and to avoid undesired light reflections. This can be controlled reducing the time exposition of the surfactant, as well as using other surfactants derivatives. In addition, a more comprehensive photophysical study is required to fully understand the energy transfer mechanism within the iridium(III) complexes in the core of the hybrid silica nanoparticles. Finally, we strongly believe that our approach can easily be extrapolated to other emitters. Here, excellent candidates are thermally stable perylene diimides derivatives that provide WHLEDs with stabilities over 500 h measured in air and on chip as recently reported by Song and Qu groups.[18] Overall, the versatility and simplicity of our new synthesis approach, as well as the excellent optical properties and stability of our hybrid nanoparticles and devices are likely to open new and exciting opportunities for the design and fabrication of new white emitters and HWLEDs.

Conflicts of interest

There are no conflicts to declare.

Acknowledgements

C. E., E. L. and J. R. B acknowledge Spanish MINECO and AEI/FEDER (ref. CTQ2016-78463-P). C. E. also thanks Universidad de La Rioja for a grant. E. F. and R.D.C. acknowledge the program “Ayudas para la atracción de talento investigador – Modalidad 1 of the Consejería de Educación, Juventud y Deporte – Comunidad de Madrid with the reference number 2016-T1/IND-1463”. R. D. C. acknowledges Spanish MINECO for the Ramón y Cajal program (RYC-2016-20891). J.G.M. acknowledges Spanish MINECO and AEI/FEDER (ref. CTQ2014-60017-R). E.S. thanks Spanish MINECO and AEI/FEDER (ref. CTQ2015-74494-JIN) and the University of Alicante (“Ayudas para la captación de talento” program with the reference number UATALENTO16-03).

Notes and references

1 J. Kido, K. Hongawa, K. Okuyama and K. Nagai, *App. Phys. Lett.*, 1994, **64**, 815-817.

2 a) D. Zhao, Z. Qin, J. Huang and J. Yu, *Org. Electron.*, 2017, **51**, 220-242; b) J. Chen, F. Zhao and D. Ma, *Mater. Today*, 2014, **17**, 175-183; c) *LG OLED* (http://www.lgoledlight.com/); d) *OLEDWorks* (https://www.oledworks.com/); e) *Konoca Minolta Pioneer* (https://www.kompo.jp/en/).

3 J. Cho, J. H. Park, J. K. Kim and E. F. Schubert, *Laser Photon. Rev.*, 2017, **11**, 1600147.

4 a) T. M. Tolhurst, S. Schmiechen, P. Pust, P. J. Schmidt, W. Schnick and A. Moewes, *Adv. Opt. Mater.*, 2016, **4**, 584-591; b) P.-P. Dai, C. Li, X.-T. Zhang, J. Xu, X. Chen, X.-L. Wang, Y. Jia, X. Wang and Y.-C. Liu, *Light Sci. Appl.*, 2016, **5**, e16024; c) W. Cheng, F. Rechberger and M. Niederberger, *ACS Nano*, 2016, **10**, 2467-2475.

5 a) *U.S. Department of Energy* (https://energy.gov/sites/prod/files/2016/06/f32/ssl_rd-plan_%20jun2016_0.pdf); b) J. Denneman, *Voice of the Lighting Industry in Europe Opens Exciting Opportunities for the European Lighting Industry*, 2016.

6 a) P. Schlotter, R. Schmidt and J. Schneider, *App. Phys. A* 1997, **64**, 417-418; b) V. Fernández-Luna, P. Coto and R. D. Costa, *Angew. Chem. Int. Ed.*, 2018, **57**, 8826-8836; c) E. Fresta, V. F. Luna, P. B. Coto and R. D. Costa, *Adv. Func. Mater.*, 2018, **28**, 1707011.

7 a) I. O. Huyal, U. Koldemir, T. Ozel, H. V. Demir and D. Tuncel, *J. Mater. Chem.*, 2008, **18**, 3568-3574; b) N. J. Findlay, J. Bruckbauer, A. R. Inigo, B. Breig, S. Arumugam, D. J. Wallis, R. W. Martin and P. J. Skabara, *Adv. Mater.*, 2014, **26**, 7290-7294; c) H. Yoo, H. S. Jang, K. Lee and K. Woo, *Nanoscale*, 2015, **7**, 12860-12867; d) C.-Y. Sun, X.-L. Wang, X. Zhang, C. Qin, P. Li, Z.-M. Su, D.-X. Zhu, G.-G. Shan, K.-Z. Shao, H. Wu and J. Li, *Nat. Commun.*, 2013, **4**, 2717; e) Y. Cui, T. Song, J. Yu, Y. Yang, Z. Wang and G. Qian, *Adv. Func. Mater.*, 2015, **25**, 4796-4802; f) D. Zhou, H. Zou, M. Liu, K. Zhang, Y. Sheng, J. Cui, H. Zhang and B. Yang, *ACS App. Mater. Interfaces*, 2015, **7**, 15830-15839; g) L. Niklaus, S. Tansaz, H. Dakhil, K. T. Weber, M. Pröschel, M. Lang, M. Kostrzewa, P. B. Coto, R. Detsch, U. Sonnewald, A. Wierschem, A. R. Boccaccini and R. D. Costa, *Adv. Func. Mater.*, 2017, **27**, 1601792; h) M. D. Weber, L. Niklaus, M. Pröschel, P. B. Coto, U. Sonnewald and R. D. Costa, *Adv. Mater.*, 2015, **27**, 5493-5498; i) L. Niklaus, H. Dakhil, M. Kostrzewa, P. B. Coto, U. Sonnewald, A. Wierschem and R. D. Costa, *Mater. Horiz.*, 2016, **3**, 340-347; j) W. Liu, Y. Fang, G. Z. Wei, S. J. Teat, K. Xiong, Z. Hu, W. P. Lustig and J. Li, *J. Am. Chem. Soc.*, 2015, **137**, 9400-9408; k) G. Meng, Z. Chen, H. Tang, Y. Liu, L. Wei and Z. Wang, *New J. Chem.*, 2015, **39**, 9535-9542; l) E.-P. Yao, Z. Yang, L. Meng, P. Sun, S. Dong, Y. Yang and Y. Yang, *Adv. Mater.*, 2017, **29**, 1606859; m) O.-H. Kim, S.-W. Ha, J. I. Kim and J.-K. Lee, *ACS Nano*, 2010, **4**, 3397-3405.

8 a) R. D. Costa, E. Ortí, H. J. Bolink, F. Monti, G. Accorsi and N. Armaroli, *Angew. Chem. Int. Ed.*, 2012, **51**, 8178-8211; b) V. K. Praveen, C. Ranjith and N. Armaroli, *Angew. Chem. Int.*

View Article Online
DOI: 10.1039/C8MH00578H

Ed., 2014, **53**, 365-368; c) E. Fred Schubert, J. Cho and J. Kyu Kim, in *Reference Module in Materials Science and Materials Engineering*, Elsevier, 2016.

9 a) X. Di, L. Shen, J. Jiang, M. He, Y. Cheng, L. Zhou, X. Liang and W. Xiang, *J. Alloy Comp.*, 2017, **729**, 526-532; b) Y. Qu, L. Feng, B. Liu, C. Tong and C. Lü, *Colloids Surf., A*, 2014, **441**, 565-571; c) F. Gai, T. Zhou, L. Zhang, X. Li, W. Hou, X. Yang, Y. Li, X. Zhao, D. Xu, Y. Liu and Q. Huo, *Nanoscale*, 2012, **4**, 6041-6049; d) M. N. Luwang, R. S. Ningthoujam, S. K. Srivastava and R. K. Vatsa, *J. Mater. Chem.*, 2011, **21**, 5326-5337; e) J. Malinge, C. Allain, A. Brosseau and P. Audebert, *Angew. Chem. Int. Ed.*, 2012, **51**, 8534-8537; f) D. Chen, G. Fang and X. Chen, *ACS App. Mater. Interfaces*, 2017; g) C. Liu, Z. Zhao, R. Zhang, L. Yang, Z. Wang, J. Yang, H. Jiang, M.-Y. Han, B. Liu and Z. Zhang, *J. Phys. Chem. C*, 2015, **119**, 8266-8272; h) H.-S. Jung, Y.-J. Kim, S.-W. Ha and J.-K. Lee, *J. Mater. Chem. C*, 2013, **1**, 5879-5884; i) M. Melucci, M. Zambianchi, G. Barbarella, I. Manet, M. Montalti, S. Bonacchi, E. Rampazzo, D. C. Rambaldi, A. Zattoni and P. Reschiglian, *J. Mater. Chem.*, 2010, **20**, 9903-9909; j) W. Nianfang, K. Sungjun, J. Byeong Guk, L. Dongkyu, K. Whi Dong, P. Kyoungwon, N. Min Ki, L. Kangha, K. Yewon, L. Baek-Hee, L. Kangtaek, B. Wan Ki and C. L. Doh, *Nanotechnology*, 2017, **28**, 185603.

10 a) C. Ezquerro, A. E. Sepulveda, A. Grau-Atienza, E. Serrano, E. Lalinde, J. R. Berenguer and J. Garcia-Martinez, *J. Mater. Chem. C*, 2017, **5**, 9721-9732; b) M. Rico, A. E. Sepulveda, S. Ruiz, E. Serrano, J. R. Berenguer, E. Lalinde and J. Garcia-Martinez, *Chem. Commun.*, 2012, **48**, 8883-8885.

11 a) D. J. Lewis, V. Dore, N. J. Rogers, T. K. Mole, G. B. Nash, P. Angeli and Z. Pikramenou, *Langmuir*, 2013, **29**, 14701-14708; b) S. Liu, J. Zhang, D. Shen, H. Liang, X. Liu, Q. Zhao and W. Huang, *Chem. Commun.*, 2015, **51**, 12839-12842; c) S. Zanarini, E. Rampazzo, L. Ciana, M. Marcaccio, E. Marzocchi, M. Montalti, F. Paolucci and L. Prodi, *J. Am. Chem. Soc.*, 2009, **131**, 2260-2267; d) S. Bonacchi, D. Genovese, R. Juris, M. Montalti, L. Prodi, E. Rampazzo and N. Zaccheroni, *Angew. Chem. Int. Ed.*, 2011, **50**, 4056-4066.

12 a) Q. Zhao, Y. Liu, Y. Cao, W. Lv, Q. Yu, S. Liu, X. Liu, M. Shi and W. Huang, *Adv. Opt. Mater.*, 2015, **3**, 233-240; b) G. Valenti, E. Rampazzo, S. Bonacchi, L. Petrizza, M. Marcaccio, M. Montalti, L. Prodi and F. Paolucci, *J. Am. Chem. Soc.*, 2016, **138**, 15935-15942; c) H. Sun, J. Zhang, K. Y. Zhang, S. Liu, H. Liang, W. Lv, W. Qiao, X. Liu, T. Yang, Q. Zhao and W. Huang, *Part. Part. Syst. Charac.*, 2015, **32**, 48-53; d) L. Donato, Y. Atoini, E. A. Prasetyanto, P. Chen, C. Rosticher, C. Bizzarri, K. Rissanen and L. De Cola, *Helv. Chim. Acta*, 2018, **101**, e1700273.

13 a) A. F. Henwood and E. Zysman-Colman, *Chem. Commun.*, 2017, **53**, 807-826; b) D. Ma, T. Tsuboi, Y. Qiu and L. Duan, *Adv. Mater.*, 2017, **29**, 1603253; c) F. Lafolet, S. Welter, Z. Popovic and L. D. Cola, *J. Mater. Chem.*, 2005, **15**, 2820-2828.

14 M. Thommes, K. Kaneko, A. V. Neimark, J. P. Olivier, F. Rodriguez-Reinoso, J. Rouquerol and K. S. W. Sing, *Pure Appl. Chemistry*, 2015, **87**, 1051-1069.

15 a) V. E. Pritchard, D. Rota Martir, E. Zysman-Colman and M. J. Hardie, *Chem. Eur. J.*, 2017, **23**, 8839-8849; b) R. Muñoz-Rodríguez, E. Buñuel, N. Fuentes, J. A. G. Williams and D. J. Cárdenas, *Dalton Trans.*, 2015, **44**, 8394-8405.

16 a) L. Grösch, Y. Lee, F. Hoffmann and M. Fröba, *Chem. Eur. J.*, 2015, **21**, 331-346; b) F. de Trindade, E. Triboni, B. Castanheira and S. Brochsztain, *J. Phys. Chem. C*, 2015, **119**, 26989-26998; c) G. Schwartz, S. Reineke, T. C. Rosenow, K. Walzer and K. Leo, *Adv. Func. Mater.*, 2009, **19**, 1319-1333.

17 a) Q. Gong, Z. Hu, B. J. Deibert, T. J. Emge, S. J. Teat, D. Banerjee, B. Mussman, N. D. Rudd and J. Li, *J. Am. Chem. Soc.*, 2014, **136**, 16724-16727; b) H. Tetsuka, A. Nagoya and R. Asahi, *J. Mater. Chem. C*, 2015, **3**, 3536-3541.

18 J. He, S. Yang, K. Zheng, Y. Zhang, J. Song and J. Qu, *Green Chem.*, 2018, **20**, 3557-3565.